

An X-Ray Free-Electron Laser Oscillator with an Energy Recovery Linac

Kwang-Je Kim and Yuri Shvyd'ko

Argonne National Laboratory, Advanced Photon Source, 9700 S. Cass Ave, Argonne, IL, 60439

Sven Reiche

UCLA, Physics and Astronomy Department, Los Angeles, CA 90095

ABSTRACT

We show that a free-electron laser oscillator generating x-rays with a wavelengths of about 1 Å is feasible using ultra-low emittance electron beams of a multi-GeV energy recovery linac, combined with a low-loss crystal cavity. The device will produce x-ray pulses with 10⁹ photons at a repetition rate of 1-100 MHz. The pulses are temporarily and transversely coherent, with an rms bandwidth of about 2 meV, and rms pulse length of about 1 ps.

An X-Ray Free-Electron Laser Oscillator with an Energy Recovery Linac

Kwang-Je Kim, Yuri Shvyd'ko

Advanced Photon Source, Argonne National Laboratory, Argonne, IL 60439, USA

Sven Reiche

UCLA, Physics and Astronomy Department, Los Angeles, CA 90095, USA

(Dated: March 25, 2008)

We show that a free-electron laser oscillator generating x-rays with a wavelength of about 1 Å is feasible using ultra-low emittance electron beams of a multi-GeV energy recovery linac, combined with a low-loss crystal cavity. The device will produce x-ray pulses with 10^9 photons at a repetition rate of 1-100 MHz. The pulses are temporarily and transversely coherent, with an rms bandwidth of about 2 meV, and rms pulse length of about 1 ps.

PACS numbers: 41.60.Cr, 41.50.+h, 42.55.Vc

In this Letter, we propose a fully coherent source of x-rays with the peak brightness comparable to that of the self-amplified spontaneous emission (SASE) from high-gain free-electron lasers (FELs) [1–3]. The average brightness is predicted to be higher by several orders of magnitudes. The key components are: a continuous sequence of ultra-low emittance electron bunches from a multi-GeV energy recovery linac (ERL)[4–6] and a low-loss optical cavity constructed from high-reflectivity crystals. The electron bunches from an ERL are not suitable for *high-gain* FELs due to its relatively small charge density. However, as we show here, an x-ray FEL is feasible in an *oscillator* configuration taking advantage of repeated low-gain amplifications. Such a device will be referred to as an x-ray FEL oscillator (X-FELO). X-FELOs can significantly enhance the capabilities of the future ERL-based x-ray facilities.

Use of crystals for X-FELO was first proposed in 1984 [7] when accelerators producing electron beams of suitable qualities were not known yet. More recently, x-ray cavity to improve the coherence of high-gain x-ray FELs was considered in [8] and studied in detail in [9]. The coherence of high-gain FEL can also be improved by a self-seeding scheme without involving an x-ray cavity [10].

The principles of an FEL oscillator are well-known [11]. A light pulse trapped in an optical cavity and an electron bunch from an accelerator meet at the entrance of an undulator and travel together. The amplified light pulse at the end of the undulator is reflected back to the entrance where it meets a fresh electron bunch, and so on. The pulse evolves from initially incoherent spontaneous emission to a coherent pulse as its intensity rises exponentially, if $(1 + g)r > 1$, where g is the gain (relative increase in the optical intensity per pass), and r is the round trip reflectivity in the cavity. The gain decreases at high intensity due to over-modulation and the system reaches a steady state, i.e., *saturates*, when $(1 + g)r = 1$.

The high reflectivity at normal-incidence required for an X-FELO cavity can be obtained by using crystals composed of low- Z atoms with high Debye temperature,

such as C (diamond), BeO, SiC, or α -Al₂O₃(sapphire), etc. [12]. As an example, Fig. 1 shows the reflectivity and transmissivity of sapphire crystals as a function of the photon energy at normal incidence to the (0 0 0 30) atomic planes for two different crystal thicknesses d . The crystal with $d=0.20$ mm is thick enough to ensure the highest reflectivity of $R = 0.96$ and thin enough to minimize the heat load due to x-ray absorption. The $d=0.07$ mm crystal will allow $T \simeq 4\%$ transmission for out-coupling of the X-FELO radiation. The crystals are assumed to be at 30 K. This ensures a high peak reflectivity, a low sensitivity of the interplanar spacing to crystal temperature, and a very high thermal conductivity. There is a valid concern about availability of high quality crystals. However, since the X-FELO beam size on the crystals will be small, about 0.2 mm in diameter, *small* high-quality single crystals seem to be feasible through selection from bulk crystals. High, almost theoretical, reflectivity in backscattering from the (0 0 0 30) atomic planes was demonstrated in the experiment on the first x-ray Fabry-Pérot interferometer [13]. An even higher reflectivity, $R \simeq 0.99$, is predicted for diamond crystals. However, diamond crystals should be used in an off normal incidence configuration to avoid losses due to the multiple beam diffraction (see [12] for more details and references).

An optical cavity for X-FELO must also provide focusing to control the intracavity mode profile. Bending the crystals is not desirable since even a very gentle bending with a curvature radius of 50 m can significantly reduce the reflectivity. A promising option is to use parabolic compound refractive lenses (CRL) [14]. Two Be parabolic CRLs, each with a radius of 0.33 mm, have a focal distance of 50 m and a very high transmissivity of $T = 0.997$, assuming surface micro-roughness less than 0.3 μm and a beam size of 0.2 mm. A grazing-incidence ellipsoidal mirror can be used to focus and also to close the loop when the Bragg mirrors are not in the exact backscattering configuration.

Three schemes for x-ray cavities are shown in Fig. 2.

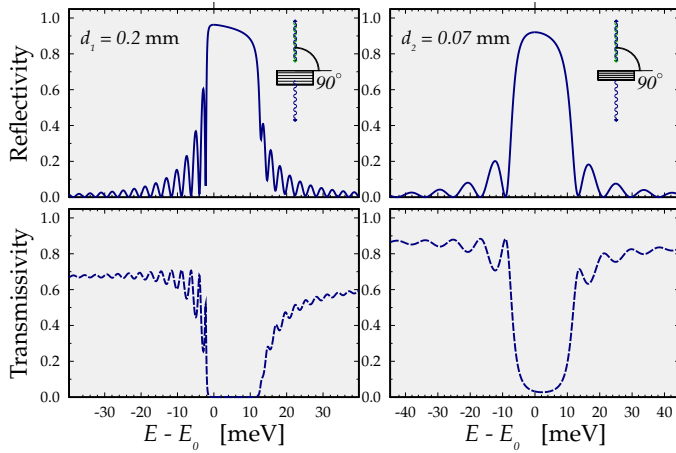


FIG. 1: Reflectivity and transmissivity of x-rays at normal incidence to the (0 0 0 30) atomic planes in α - Al_2O_3 . Crystal temperature $T = 30$ K, $E_0 = 14.326$ keV. The calculations have been performed using dynamical diffraction theory with the crystal data as in [12].

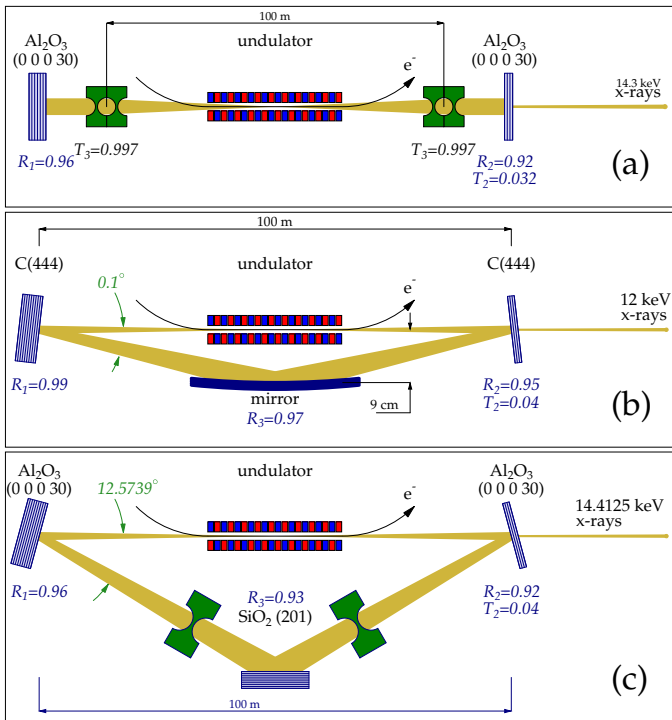


FIG. 2: Schemes of x-ray cavities.

Scheme (a) is a two-bounce system using the two normal-incidence sapphire crystals with reflectivities as in Fig. 1, and the CRLs. Scheme (b) uses two diamond crystals with the (444) Bragg reflection slightly off from the exact backscattering for 12.04-keV x-rays. A grazing-incidence ellipsoidal mirror focuses the beam and closes the loop. Scheme (c) is designed specially for $E = 14.4125$ keV photons for nuclear resonance scattering experiments

with ^{57}Fe [15]. It uses two sapphire crystals at an angle of incidence of 6.287° , the (201) reflection from a SiO_2 crystal closes the loop, and CRLs are used for focusing. Taking into account all losses from crystals and focusing elements, the round-trip peak reflectivities are 87%, 91%, and 81% for Schemes (a), (b), and (c), respectively. With these reflectivities the XFEL-O can operate if $g \gtrsim 30\%$. In all these cases, the out coupling fraction is about 4%.

Out of several possible operating modes of an ERL [4], the *high coherence* mode is best suited for an X-FELO. The bunch parameters in this mode are: charge $Q = 19$ pC, normalized transverse emittance $\varepsilon_{\text{nx}} = 0.82 \times 10^{-7}$ m, rms energy spread $\sigma_{\Delta E} = 1.4$ MeV, and rms length $\tau_{\text{el}} = 2$ ps. These beam parameters are assumed to be the same for the 7-GeV APS ERL [6], since they are invariant under acceleration. The value of ε_{nx} is smaller by about one order of magnitude than that achieved for high-gain FELs [16]. However, we can be optimistic about achieving a smaller emittance since the peak current in our case is smaller by almost three orders of magnitude. An optimization study of a laser-driven, high-voltage DC gun shows that the bunch parameters listed above are feasible for $19 \text{ pC} \leq Q \leq 60 \text{ pC}$ [17].

The X-FELO performance was studied by analytical calculation and by simulation using the GENESIS code [18]. Since guiding can be neglected for a low-gain FEL, we assume that the FEL mode in the cavity is Gaussian with the waist at the center of the undulator. For the electron beam, we assume that focusing is absent, the distribution is Gaussian, and the envelope parameter at the waist β^* is the same as the Rayleigh length Z_R of the FEL mode. The gain formula in reference [19] can then be reduced to an expression involving a double integral that can be easily evaluated. The intracavity power at saturation P_{sat} is determined by GENESIS simulation to be the power at which $(1 + g)r = 1$.

Table I gives some X-FELO examples. The beam parameters ε_{nx} , $\sigma_{\Delta E}$, and τ_{el} are assumed to be those listed above. The undulator parameters are: K -deflection parameter, λ_U -undulator period, N_U -number of periods, and $L_U = N_U \lambda_U$ -undulator length. The wavelength for the fundamental FEL harmonic is $\lambda_1 = (1 + K^2/2)\lambda_U/2\gamma^2$ where γ is the electron energy E divided by the electron's rest energy. The undulators in the table can all be constructed using steel poles and Ne-Fe-B magnets with a gap of 5 mm [20]. The values of $Z_R = \beta^*$ given in the table are that corresponding to the maximum gain; it is about 10 m for the cases studied here. The low-power gain computed analytically, g_{th} , and by simulation, g_{sim} , agree reasonably well. The last two rows of the table show that the gain is higher at higher energy since both the geometrical emittance and the relative energy spread become smaller. As shown later in the discussion of the temporal mode structure, the rms length of the x-ray pulse is about 0.85 ps. Assuming 4% output coupling, each output pulse then contains 0.9×10^9

photons.

We have assumed a straight undulator in the above. Higher gain may be possible with an optical klystron configuration [21]. Also, the polarization of the X-FELO can be modulated arbitrarily by employing a crossed undulator configuration proposed in [22] and demonstrated recently [23]. In the above, we have concentrated on photon energies 12 keV or higher. X-FELOs at lower energies will be easier to design since the requirement on electron emittance is relaxed and both sapphire and diamond have high reflectivities at lower energies down to about 5 keV.

To study the mode evolution of the X-FELO, GENESIS code was modified to add propagation in free space between the undulator and the mirrors, frequency filtering and reflection by mirrors, and focusing. To reduce the CPU time, a short time window of 25 fs was chosen. The resulting frequency bandwidth is larger than the bandwidth of the crystals, and thus only one frequency component is present after reflection. Therefore, the wavefront is the same over the entire time window, and only one single wavefront needs to be propagated. Even with this simplification, simulation of a single pass took about two hours with a 25-node computer cluster at UCLA. A full tracking from initial spontaneous emission to final saturation took about one month. Figure 3 shows the power as a function of the pass number. One sees that an exponential growth emerges from the initial randomness after about 100 passes.

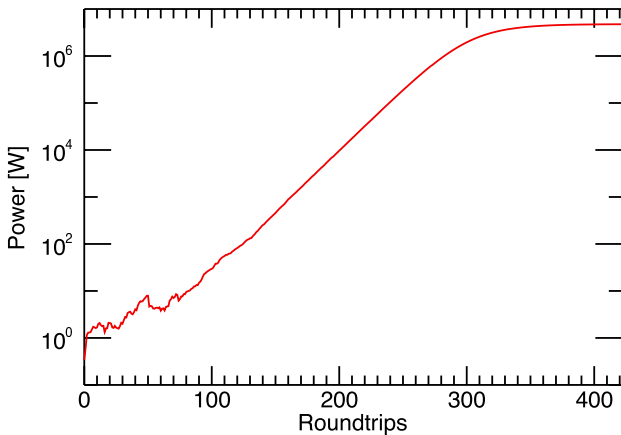


FIG. 3: Evolution of intracavity peak power for the case corresponding to the first row in Table I.

The temporal structure of the mode can be studied by adapting the supermode analysis [24, 25] to the case of a narrow cavity bandwidth. Let τ_{el} and τ_{opt} be the rms lengths of the electron bunch and optical mode, respectively. We also introduce the length $\tau_M = (\omega/\sigma_\omega^M)(\lambda/4\pi c) = 1/2\sigma_\omega^M$ corresponding to the rms frequency bandwidth of the optical cavity σ_ω^M . We neglect the slippage effect since the total slippage length $\tau_s = N_U\lambda/c$ is about 1 fs which is smaller than all other

length scales. Suppressing the transverse dependence, the electric field amplitude at the end of the undulator at the n^{th} pass can be written as $a(n, \zeta) \exp(i\omega\zeta)$, where $\zeta = t - z/c$ is the time coordinate relative to the bunch center and $a(n, \zeta)$ is the slowly varying part of the amplitude. Upon reflection by the crystals, the amplitude is filtered in frequency domain and becomes, assuming $\tau_{\text{opt}} \gg \tau_M$, $a_M(n, \zeta) \approx a(n, \zeta) + \tau_M^2 a(n, \zeta)''$, where the prime denotes $d/d\zeta$. The pulse is then displaced in time by u with respect to a fresh electron beam, and amplified. For simplicity we neglect the imaginary part of gain and write the amplitude gain as $0.5gU(\zeta)$, where $U(\zeta) = 1 - \zeta^2/(2\tau_{\text{el}}^2)$ is a factor representing the electron density fall-off assuming $\tau_{\text{el}} \gg \tau_{\text{opt}}$. Also taking into account the loss $\alpha = 1 - r$, the amplitude at the $(n+1)^{\text{th}}$ pass is $a(n+1, \zeta) = (1 + (gU(\zeta) - \alpha)/2)a_M(n, \zeta + u)$. By expanding in u and retaining only the lowest terms,

$$\frac{\partial a_n(\zeta)}{\partial n} = \left(\frac{1}{2}(g - \alpha) + u \frac{\partial}{\partial \zeta} + \tau_M^2 \frac{\partial^2}{\partial \zeta^2} - \frac{g}{4\tau_{\text{el}}^2} \zeta^2 \right) a_n(\zeta). \quad (1)$$

The solution of this equation is $a_n(\zeta) = \exp[n\Lambda_m - u\zeta/(2\tau_M^2) - g^{1/2}\zeta^2/(4\tau_M\tau_{\text{el}})]H_m(g^{1/4}\zeta/\sqrt{2\tau_{\text{el}}\tau_M})$, where $H_m(x)$ is the Hermite polynomial, and the growth rate per pass is

$$\Lambda_m = (g - \alpha)/2 - (u/2\tau_M)^2 - 0.5\sqrt{g}(2m+1)(\tau_M/\tau_{\text{el}}). \quad (2)$$

The fundamental mode $m = 0$ has the largest growth rate with a Gaussian profile, with the rms length $\tau_{\text{opt}} = \sqrt{2\tau_{\text{el}}\tau_M}/g^{1/4}$, corresponding to the bandwidth $\sigma_\omega^{\text{opt}} = 1/2\tau_{\text{opt}} = g^{1/4}/\sqrt{8\tau_{\text{el}}\tau_M}$.

From Fig.1, the full spectral width of a single crystal is about 10 meV. Thus the rms width of two crystals forming the optical cavity can be estimated as $\hbar\sigma_\omega^M = 10/\sqrt{4\pi} = 2.8$ meV. Taking $g = 0.3$ and $\tau_{\text{el}} = 2$ ps, we obtain $\tau_M = 0.1$ ps, $\tau_{\text{opt}} = 0.85$ ps, and $\hbar\sigma_\omega^{\text{opt}} = 2.3$ meV.

To limit the reduction in the effective gain by the second term in Eq.(2) to within 1%, we require $u < 0.2\tau_M$, which becomes $u < 20$ fs in the present case. The tolerance in the timing of the electron beam is therefore 20 fs, and the corresponding tolerance in the optical cavity length is 3 μm . The angular tolerance $\Delta\theta$ of the mirror may be determined by requiring that the change of the optical axis of the cavity be less than one tenth of the rms mode angle. We obtain $\Delta\theta \leq 0.8(Z_R/L_{\text{opt}})^2\sqrt{\lambda/2LU}$, where L_{opt} is the length of the optical cavity. Taking $L_{\text{opt}} \simeq 100$ m, we find $\Delta\theta \leq 8$ nrad. These tolerances are tight but should be achievable.

The GENESIS calculation shows that the rms energy spread of the electron beam increases from 0.02% to 0.05% due to the FEL interaction. Such an increase can be accommodated by the ERL return pass since the fractional loss of particles is well below the 1×10^{-4} level with the increased energy spread [26].

With $L_{\text{opt}} \simeq 100$ m, the repetition rate of X-FELO output is about 1.5 MHz, if a single optical pulse is stored

TABLE I: Performance of X-FELO. See text for explanation of symbols

λ_1 (Å)	E (GeV)	Q (pC)	K	λ_U (cm)	N_U	Z_R (m)	g_{th} (%)	g_{sim} (%)	r (%)	P_{sat} (MW)
1	7	19	1.414	1.88	3000	10	26	28	90	19
1	7	40	1.414	1.88	3000	12	55	66	83	21
0.84	7.55	19	1.414	1.88	3000	12	26	28	90	20
0.84	10	19	2	2.2	2800	10	42	45	83	18

in the cavity. The upper limit of the repetition rate is determined by the heat load on the crystals. The average power and power density incident on the 100- μ m radius hot spot receiving the coherent x-rays are about 21 W and 2 kW/mm², respectively. These can be compared to a 5 – 10 kW total power and typical power density of 2 kW/mm² of the undulators at the 3rd generation sources. Therefore, a higher repetition rates, perhaps 100 MHz, might be feasible.

Compared to SASE from a high gain FEL, the pulse intensity of an X-FELO is lower by two or three orders of magnitude, but its spectrum is narrower by more than three orders of magnitude. The pulse repetition rate is at least $\simeq 1$ MHz, which is higher by at least two orders of magnitude than that of the high-gain, high-repetition-rate FEL using a super-conducting linac[2]. The average spectral brightness of an X-FELO will be 10^{26} (10^{28}) photons/sec/(mm-mr)²(0.1% BW) assuming 1(100) MHz repetition rate.

With full coherence, extremely narrow bandwidth $\simeq 2$ meV, and polarization control, X-FELOs for x-rays in the range from 5 keV to 20 keV may open up new scientific opportunities in various research fields, such as inelastic scattering [27] nuclear resonance scattering [15], x-ray imaging, and bulk-sensitive hard x-ray photoemission spectroscopy [28]. In particular, time-resolved measurement of Fermi surfaces via angle-resolved photo-emission spectroscopy could be possible [29].

ACKNOWLEDGEMENTS

We thank Yusong Wang for his help with the GENE-SIS simulation, Ali Khounsary for discussions on thermal loading, and Fulvio Parmigiani for enthusiastic discussions on X-FELO applications. The research at Argonne is supported by the U.S. Department of Energy, Office of Science, Office of Basic Energy Sciences, under Contract No. DE-AC02-06CH11357.

[1] LCLS Conceptual Design Report, SLAC-R-593 (2002).

[2] R. Brinkmann, Proc. of FEL06, 24 (2006); <http://www.jacow.org>.

- [3] T. Tanaka, Y. Asano, H. Baba et al., Proc. of FEL05, 75 (2005); <http://www.jacow.org>.
- [4] D. H. Bilderback, C. Sinclair, and S. M. Gruner, Synch. Rad. News **19-6**, 30 (2006).
- [5] T. Kasuga, Proc. of APAC07, 172 (2007); <http://www.jacow.org>.
- [6] M. Borland, G. Decker, A. Nassiri, and M. White, Proc. of PAC07, 1121 (2007); <http://www.jacow.org>.
- [7] R. Colella, and A. Luccio, Opt. Commun. **50**, 41 (1984).
- [8] B. Adams and G. Materlik, *Proc. of Free Electron Lasers 1996*, II-24 (North Holland, Amsterdam, 1997).
- [9] Z. Huang and R. Ruth, Phys. Rev. Lett. **96**, 144801 (2006).
- [10] E. L. Saldin, E. A. Schneidmiller, Yu. V. Shvyd'ko, and M. V. Yurkov, Nucl. Instrum. Methods A **475**, 375 (2001).
- [11] See, for example, C. Brau, *Free-Electron Lasers*, (Academic Press, San Diego, 1990).
- [12] Yu. Shvyd'ko, *X-Ray Optics – High-Energy-Resolution Applications*, Berlin Heidelberg New York, 2004).
- [13] Yu. V. Shvyd'ko, M. Lerche, H.-C. Wille, E. Gerdau, E. E. Alp, M. Lucht, H. D. Rüter, and R. Khachatryan, Phys. Rev. Lett. **90**, 013904 (2003).
- [14] B. Lengeler, C. Schroer, J. Tümmler, B. Benner, M. Richwin, A. Snigirev, I. Snigireva, and M. Drakopoulos, J. Synchrotron Rad. **6**, 1153 (1999).
- [15] E. Gerdau and H. de Waard, eds., *Nuclear Resonant Scattering of Synchrotron Radiation* (Baltzer, 1999/2000), special issues of the *Hyperfine Interact.*, Vol. 123-125.
- [16] R. Akre, et al. Phys. Rev. ST Accel. Beams, **to be published** (2008).
- [17] I. V. Bazarov and C. K. Sinclair, Phys. Rev. ST Accel. Beams **8**, 034202 (2005).
- [18] S. Reiche, Nucl. Instrum. Methods A **429**, 243 (1999).
- [19] K.-J. Kim, Nucl. Instrum. Methods A **318**, 489 (1992).
- [20] K. Halbach, J. de Phys. **44**, C1-211 (1983).
- [21] N. A. Vinokurov, Proc. 10th Int. Conf. on High Energy Particle Accel. **2**, 454 (1977).
- [22] K.-J. Kim, AIP Conf. Proc. **118**, 229 (1984).
- [23] Y. Wu, Phys. Rev. Lett. **96**, 224801 (2006).
- [24] G. Dattoli A. Marino, A. Renieri, and F. Romanelli, IEEE J. Quant. Elect. **QE-17**(8), 1371 (1981).
- [25] P. Elleaume, IEEE J. Quant. Elect. **QE-21**(7), 1012 (1985).
- [26] M. Borland, private communications.
- [27] E. Burkel, Rep. Prog. Phys. **63**, 171 (2000).
- [28] G. Paolicelli, et al., J. Electron Spectroscopy **144-147**, 963 (2005).
- [29] F. Parmigiani, private communications.